

# Counting gamma rays in the directions of galaxy clusters.

D. A. Prokhorov<sup>1</sup>, E. M. Churazov<sup>1,2</sup>

<sup>1</sup> Max Planck Institute for Astrophysics, Karl-Schwarzschild-Strasse 1, 85741 Garching, Germany

<sup>2</sup> Space Research Institute (IKI), Profsovnaya 84/32, Moscow 117997, Russia

Accepted . Received ; Draft printed: September 3, 2013

## ABSTRACT

Emission of AGNs and neutral pion decay – are the two most natural mechanisms, that could make a galaxy cluster be a source of gamma-rays in the GeV regime. We revisited this problem by using 52.5-month FERMI-LAT data above 10 GeV and stacking 55 clusters from the HIFLUGS sample of the X-ray brightest clusters. The choice of >10 GeV photons is optimal from the point of view of angular resolution, while the sample selection optimizes the chances of detecting signatures of the neutral pion decay, arising from hadronic interactions of relativistic protons with an intra-cluster medium, which scale with the X-ray flux. In the stacked data we detected a signal for the central 0.25 deg circle at the level of 4.3  $\sigma$ . An evidence for a spatial extent of the signal is marginal. A subsample of cool-core clusters has higher count rate  $1.9 \pm 0.3$  per cluster compared to the subsample of non-cool core clusters  $1.3 \pm 0.2$ . Several independent arguments suggest that the contribution of AGNs to the observed signal is substantial if not dominant. No strong support for the large contribution of pion decay was found. In terms of a limit on the relativistic protons energy density, we got an upper limit of  $\sim 1.5\%$  relative to the gas thermal energy density, provided that the spectrum of relativistic protons is hard ( $s=4.1$  in  $dN/dp=p^{-s}$ ). This estimate assumes that relativistic and thermal components are mixed. For softer spectra the limits are weaker.

**Key words.** Galaxies: clusters: general; Gamma rays: galaxies: clusters; Radiation mechanisms: non-thermal

## 1. Introduction

Galaxy clusters are megaparsec-scale structures that consist of hundreds of galaxies and high temperature,  $T_{\text{gas}} \approx 10^7 - 10^8$  K, sparse highly ionized plasmas filling the space between galaxies (for a review, see Sarazin 1986). X-ray radiation via bremsstrahlung and via ionic emission lines from intracluster plasmas has permitted to study thermal components of the intra-cluster medium (ICM). It has been shown that galaxies and plasmas in a galaxy cluster are gravitationally bound to its dark matter halo. The constraints on non-thermal components in galaxy cluster cores can be obtained from a comparison of gravitational potential profiles derived from X-ray and optical data (e.g., see Churazov et al. 2008). Detection of diffuse radio emission from many galaxy clusters provided the strong evidence of the presence of relativistic electrons with very high energies (with a Lorentz factor of  $\gamma \sim 10^3$ ), emitting through the synchrotron mechanism in magnetic fields of the ICM (for a review, see Ferrari et al. 2008). The interaction of relativistic electrons of such energies with cosmic microwave background (CMB) photons may result in hard X-ray emission via the Inverse Compton (IC) process, while the IC emission owing to the interaction of more energetic electrons,  $\gamma > 10^5$ , with CMB photons may lead to gamma-ray emission (e.g., see Petrosian et al. 2008).

By analogy with the relativistic particle composition in the Milky Way galaxy, one can assume that relativistic protons are also present in galaxy clusters. The collisions of relativistic protons with thermal protons may result in gamma-ray emission via the decay of neutral pions produced in these inelastic proton-proton collisions (e.g., see Dermer 1986). The candidates as sources of electrons and protons of very high energies in galaxy clusters are active and normal galaxies, and structure formation

shocks (e.g., see Berezhinsky et al. 1997). The lifetime of high energy protons,  $E > 10$  GeV, in galaxy clusters exceeds the Hubble time (e.g., see Völk et al. 1996), but the lifetime of very high energy electrons with  $\gamma \sim 10^5$ , which emit gamma-rays via the IC effect, in the ICM is several orders of magnitude less than the Hubble time (e.g., see Petrosian et al. 2008). Observations of diffuse radio emission from galaxy clusters hosting radio halos indicate that electrons with  $\gamma \sim 10^3$  are continuously produced in the ICM and that acceleration mechanisms overtake the electron energy losses (e.g., Brunetti & Lazarian 2007). Note that gamma-rays produced in annihilation of hypothetical dark matter particles, such as WIMPs, can potentially contribute to emission from galaxy clusters (e.g., see Ackermann et al. 2010b).

Clusters of galaxies, which are bright extended X-ray sources, are promising targets for gamma-ray telescopes (e.g., see Michelson et al. 2010), but an observational evidence that gamma-rays are emitted by galaxy clusters is still at large. Energetic Gamma Ray Experiment Telescope (EGRET) was collecting data on gamma rays (ended in June 2000) ranging from 30 MeV to 30 GeV (for a review, see Thompson 2008) and its successor, *Fermi* Large Area Telescope (LAT), is collecting the data covering the energy range from 20 MeV to more than 300 GeV (Atwood et al. 2009) (the science phase of the *Fermi* mission began on 2008 August 4). The analyses of the EGRET data (Reimer et al. 2003) and of the first 18 months of *Fermi*-LAT data (Ackermann et al. 2010a) have allowed to put the flux upper limits on gamma-ray emission from individual galaxy clusters. The predicted gamma-ray fluxes from clusters are not strongly below than the observed flux upper limits (Pinzke & Frommer 2010) and this suggests that a stacking analysis should be a powerful tool to search of gamma-rays from galaxy clusters (e.g., see Zimmer et al. 2011; Dutson et al. 2013).

At 10 GeV, *Fermi*-LAT provides an increase in effective area over EGRET on an order of magnitude. Note that the

Send offprint requests to: D.A. Prokhorov e-mail: phdmi try@mpa-garching.mpg.de

AntiCoincidence Detector, ACD, of EGRET was monolithic, which caused problems above 10 GeV: electromagnetic showers in the calorimeter produced backscatter which made a signal in the ACD, thus tagging high energy gamma-rays incorrectly as charged particles. To avoid this effect, the ACD for *Fermi*-LAT is divided into many scintillating tiles (see Moiseev et al. 2007) and, therefore, *Fermi*-LAT provides us with a unique opportunity to study incoming gamma-rays with energies above 10 GeV. At energies below  $\approx 10$  GeV, the accuracy of the directional reconstruction of photon events detected by *Fermi*-LAT is limited by multiple scattering, whereas above  $\approx 10$  GeV, multiple scattering is unimportant and the accuracy is limited by the ratio of silicon-strip pitch to silicon-layer spacing (see Atwood 2007).

In this paper, we perform a search for gamma-ray emission from a sample of galaxy clusters with modest angular sizes by analyzing the data from *Fermi*-LAT. For this purpose, we stack photons with GeV energies coming from the regions covering clusters of galaxies. The theoretical argument that gamma-ray photon spectra of galaxy clusters are harder (e.g., see Miniati 2003) than that of the galactic and extragalactic diffuse emission (e.g., see Abdo et al. 2010; Ackermann et al. 2012b) provides us with lower background at high energies than that those at lower energies and, therefore, provides a higher signal-to-noise ratio at high energies. This argument holds for both the mechanisms of gamma-ray production (i.e., via the IC effect and via neutral pion decay). The fine (0.228 mm) pitch of the strips, applied in *Fermi*-LAT, gives excellent angular resolution for high energy photons. The point spread function of *Fermi*-LAT strongly depends on photon energy and the 68% angle containment radius significantly decreases with energy (from  $\approx 5^\circ$  at 100 MeV to  $\approx 0.2^\circ$  at 10 GeV, Ackermann et al. (see 2012a)). This allows us to associate more precisely the observed photons above 10 GeV with those that should come from clusters of galaxies, and is especially important for galaxy clusters with an angular size smaller than a degree. This precise association permits us to perform a temporal analysis for testing the variability of gamma-ray sources in the directions of galaxy clusters. Below we demonstrate that the number of high energy photons is sufficient in order to search a statistically significant signal from galaxy clusters and that our analysis reveals a tentative excess of gamma rays in the direction of galaxy clusters. Comparing the positions of galaxy clusters in the sky with those of expected gamma-ray blazar sources from the CGRaBS catalogue (see Healey et al. 2008), we exclude eight galaxy clusters possibly associated with CGRaBS gamma-ray candidate sources and put the upper limit on relativistic-hadron-to-thermal energy density ratio using a sample of 47 galaxy clusters.

## 2. Observation and data reduction

The *Fermi*-LAT, the primary scientific instrument on the Fermi Gamma Ray Space Telescope spacecraft, is an imaging high-energy gamma-ray pair conversion telescope covering the energy range from about 20 MeV to more than 300 GeV (Atwood et al. 2009). Tungsten foils and silicon microstrip detectors are applied to convert incoming photons into electron-positron pairs and to measure the arrival direction of gamma-rays. A cesium iodide hodoscopic calorimeter is used to provide an energy measurement of the electron-positron pairs. The Fermi spacecraft travels in an almost circular near-Earth orbit at an altitude of 550 km with a period of about 96 minutes. The field-of-view of *Fermi*-LAT covers about 20% of the sky at any time, and it scans continuously, covering the whole sky every three hours (two orbits). By using the silicon strip technique with

tungsten convertors (instead of the spark chamber technique), *Fermi*-LAT achieves a finer precision in the measurement of the directions of incoming gamma-rays than that of EGRET. The description of the current instrument performance can be found in Ackermann et al. (see 2012a).

We use the first 52.5 months of the *Fermi*-LAT data, collected between 2008-08-04 and 2012-11-29 and perform the data analysis using the Fermi Science Tools v9r27p1 package<sup>1</sup>. “Source” class events, which are recommended for an analysis of gamma-ray point sources<sup>1</sup> (including events converted in both the front and back sections of the LAT tracker) with energies between 10 GeV and 270 GeV are selected. Events with zenith angles larger than  $100^\circ$  are rejected to minimize contamination from gamma-rays from the Earth limb. We removed events that occur during satellite maneuvers when the LAT rocking angle was larger than  $52^\circ$ . Time intervals when some event has negatively affected the quality of the LAT data are excluded. We select events in a circular region of interest of  $4^\circ$  radius around each galaxy cluster specified below.

The selection of photon events with  $E > 10$  GeV for our counting experiment relies on a higher signal-to-noise ratio (S/N) expected in this energy band compared with that at energies of  $E > 200$  MeV and  $E > 1$  GeV. The S/N for a point-like source observed against isotropic background is given by

$$(S/N)_E \propto N_{src}(E) \times \sqrt{\frac{A_{eff}(E)}{I_{bkg} \times \Sigma}}, \quad (1)$$

where  $N_{src}(E)$  is a number of incoming photons with energies,  $>E$ , from the source,  $A_{eff}(E)$  is an effective area of the detector as a function of energy,  $I_{bkg}$  is an intensity of background emission, and  $\Sigma$  is surface area corresponding to the 68% angle containment radius at energy,  $E$ . Thus one expects the following improvement of the S/N using  $E > 10$  GeV instead of  $E > 200$  MeV

$$\frac{(S/N)_{10\text{GeV}}}{(S/N)_{0.2\text{GeV}}} \approx \left(\frac{10}{0.2}\right)^{-2.1+1} \sqrt{\frac{0.77}{0.42} \times \left(\frac{10}{0.2}\right)^{(2.4-1)} \left(\frac{3}{0.25}\right)} \approx 3.4, \quad (2)$$

and using  $E > 10$  GeV instead of  $E > 1$  GeV

$$\frac{(S/N)_{10\text{GeV}}}{(S/N)_{1\text{GeV}}} \approx \left(\frac{10}{1}\right)^{-2.1+1} \sqrt{\frac{0.77}{0.68} \times \left(\frac{10}{1}\right)^{(2.4-1)} \left(\frac{0.9}{0.25}\right)} \approx 1.5, \quad (3)$$

where 0.42, 0.68, and 0.77  $\text{m}^2$  are the approximate values of effective area at 0.2, 1, and 10 GeV for normal incidence photons; 3.0, 0.9, and 0.25 $^\circ$  are the approximate values of the 68% angle containment radius at 0.2, 1, and 10 GeV (Ackermann et al. 2012a); and 2.1 and 2.4 are power-law photon indices for a point source and isotropic background emission, respectively. The spectral analysis of gamma-ray observations of galaxy clusters performed in several energy bins will be presented in Sect. 4 to clarify the importance of observed photons with energies of several GeV, for a detection of gamma-ray sources with hard spectra.

As mentioned in Sect. 1, X-ray astronomy has provided a perfect tool to detect massive galaxy clusters through imaging and spectroscopy. ROSAT All-Sky X-ray Survey (RASS; Truemper (1993); Voges et al. (1999)) have been performed for the purpose of searching for X-ray sources. A highly complete flux limited sample of the X-ray brightest galaxy clusters (HIFLUGCS,

<sup>1</sup> <http://fermi.gsfc.nasa.gov/ssc/data/analysis/>

the Highest X-ray FLUX Galaxy Cluster Sample) has been published by Reiprich & Böhringer (2002). Since the gamma-ray luminosities of galaxy clusters are expected to increase with a cluster mass (e.g., see Pinzke & Pfrommer 2010) and the X-ray luminosities of galaxy clusters increase with a cluster mass, accordingly to the X-ray luminosity–mass relation (e.g., see Hoekstra et al. 2011), we use the HIFLUGCS catalogue to select a sample of galaxy clusters for our analysis of the gamma-ray data. Note that galaxy clusters from the HIFLUGCS sample are located at high galactic latitudes,  $|b| > 20^\circ$ . Therefore, the selection of these clusters for a gamma-ray analysis minimizes contamination of a gamma-ray signal from galaxy clusters by diffuse galactic emission which dominates at low galactic latitudes.

The HIFLUGCS catalogue includes fifty seven galaxy clusters with angular sizes (defined by the ratio of the virial radius to the distance) smaller than  $1^\circ$ . These galaxy clusters are targets of our study. The selection of galaxy clusters with high X-ray fluxes from this catalogue provides us with a suitable sample of galaxy clusters to constrain gamma-ray emission, produced via neutral pion decay, using the proportionality of X-ray and gamma-ray fluxes expected in this model (see, e.g., Ensslin et al. 1997). The redshifts of these 57 galaxy clusters lie in the interval of  $0.016 < z < 0.2$  (only one cluster lies at  $z > 0.1$ ) and their X-ray fluxes (in the energy range of 0.1–2.4 keV) are in the interval of  $(2.0\text{--}12.1) \times 10^{-11} \text{ erg s}^{-1} \text{ cm}^{-2}$ . This catalogue also contains several groups and clusters of galaxies with large angular sizes exceeding  $1^\circ$ , namely Fornax, Hydra, Coma, NGC4636, Centaurus, and NGC5044. Although these six extended objects are ones of the nearest and, therefore, their fluxes are relatively high, we do not include them in the present analysis. This is because their large angular extensions can make problematic to take into account a possible population of extragalactic gamma-ray point sources (e.g., blazars), that can contribute to gamma-ray signals towards these clusters. Possible inhomogeneities of galactic diffuse emission in the direction of the extended clusters requires a supplementary analysis. The nearby Fornax, Coma, and Centaurus clusters of galaxies are promising targets for gamma-ray studies in order to constrain the parameters of the hadronic cosmic ray model and of some dark matter annihilation models (e.g., Zimmer et al. 2011; Ando & Nagai 2012).

A gamma-ray signal from clusters of galaxies can be contaminated by various point gamma-ray sources, e.g. blazars, that occasionally located near galaxy clusters in the sky. To minimize contamination of a signal from galaxy clusters, we explore the LAT 2-year Point Source Catalog (the 2FGL catalogue, Nolan et al. 2012) searching for point gamma-ray sources located near the clusters of galaxies from the HIFLUGCS catalogue and detected by the *Fermi*-LAT in the first two years of the mission. The search shows that there are gamma-ray sources from the 2FGL catalogue near the positions of two galaxy clusters (namely, Abell 3376 and Abell 2589). The 2FGL catalogue names of these gamma-ray sources are 2FGL J0602.7-4011 (which lies at the distance of  $\approx 0.26^\circ$  from the center of Abell 3376) and 2FGL J2325.4+1650 (which lies at the distance of  $\approx 0.37^\circ$  from the center of Abell 2589). The gamma-ray source 2FGL J2325.4+1650 is associated with the radio source NVSS J232538+164641 in Nolan et al. (2012), while 2FGL J0602.7-4011 is an unidentified gamma-ray source.

To check if these two 2FGL sources can possibly be identified with galaxy clusters, we estimate the flux at  $E > 200 \text{ MeV}$  from each of these 2FGL gamma-ray sources using their fluxes at  $E > 1 \text{ GeV}$  and spectral indices listed in the 2FGL catalogue. The calculated fluxes at  $E > 200 \text{ MeV}$  are  $6.5 \times 10^{-9}$  and  $2.4 \times 10^{-9}$

$\text{ph cm}^{-2} \text{ s}^{-1}$  for 2FGL J0602.7-4011 and 2FGL J2325.4+1650, respectively, and are not much lower than the  $2\sigma$  flux upper limit of  $4.58 \times 10^{-9} \text{ ph cm}^{-2} \text{ s}^{-1}$  at  $E > 200 \text{ MeV}$  for the Coma cluster (taken from Ackermann et al. (2010a)). We use the proportionality relation between X-ray and gamma-ray fluxes (expected for gamma-ray emission via pion decay, see e.g., Ensslin et al. (1997)), to test the possible identification of these two 2FGL sources with A3376 and A2589. The X-ray fluxes for A3376, A2589, and Coma are taken from Reiprich & Böhringer (2002)) and are equal to  $4.6 \times 10^{-11}$ ,  $4.7 \times 10^{-11}$ , and  $6.4 \times 10^{-10} \text{ erg cm}^{-2} \text{ s}^{-1}$ , respectively. Taking into account the observed X-ray fluxes and plasma temperatures of A3376, A2589, and Coma, we found that the expected gamma-ray flux from the Coma cluster is about twenty times greater than those expected from A3376 and A2589 when the same relativistic-hadron-to-thermal energy density ratio is assumed. Since the observed gamma-ray fluxes at  $E > 200 \text{ MeV}$  from these 2FGL sources are not twenty times lower than the flux upper limit for the Coma cluster, we conclude that the upper limit on relativistic-hadron-to-thermal energy density ratio obtained from the analysis of the Coma cluster cannot be incorporated with the hypotheses that 1) gamma-rays from 2FGL J0602.7-4011 and 2FGL J2325.4+1650 are produced via neutral pion decay emission in A3376 and A2589 and that 2) the relativistic-hadron-to-thermal energy density ratio in A3376 and A2589 does not exceed the upper limit derived from the analysis of the Coma cluster.

There are  $\approx 1000$  BL Lac object type of blazars, FSRQ type of blazars, and other active galactic nuclei in the 2FGL catalogue. Assuming that these objects are isotropically distributed in the sky, the expected number of galaxy clusters having one of such 2FGL gamma-ray point sources within the circle of  $0.4^\circ$  is  $\approx 0.7$  and it is in agreement with the fact that there are two galaxy clusters from the sample of 57 clusters in the vicinity of one of 2FGL point gamma-ray sources in the sky. Though the possible association of a gamma-ray source with the cluster Abell 3376 is of interest particularly in the light of the ring-shaped nonthermal radio-emitting structures discovered in the outskirts of this cluster (Bagchi et al. 2006) and of the expectation of a strong gamma-ray signal from the outer shock waves of Abell 3376 (e.g. Araudo et al. 2008), we withdraw Abell 3376 and Abell 2589 from the sample of the clusters of galaxies selected for the present analysis.

Apart from the point sources located in the close vicinity of galaxy clusters in the sky, there are point sources within the  $4^\circ$  regions of interest around each cluster. These point sources should be taken into account in order to estimate diffuse background emission. The four brightest of these sources included in the 2FGL catalogue, namely 2FGLJ0710.5+5908, 2FGLJ1256.1-0547, 2FGLJ1522.1+3144, and 2FGLJ1800.5+7829, are strong at energies higher 10 GeV. These four sources are associated with blazars, RGB J0710+591, 3C 279, B2 1520+31, and S5 1803+784, respectively. The test-statistics values (Mattox et al. 1996) of these four blazars are larger than 100 at  $E > 10 \text{ GeV}$  accordingly the 2FGL catalogue. Since the test-statistics is extensive, one can expect that the test-statistics will be larger 200 for each of these four blazars when the first 52.5 months of the *Fermi*-LAT data are analyzed. Thus, e.g., the expected TS value will be equal to 560 for the blazar 2FGLJ1256.1-0547, if we assume that this source is unvariable in time. Dividing the expected TS value by the number of the selected regions of interest (i.e., 55), one can expect that this blazar will appear at the stacked image as a source with the confidence level of  $\approx 3\sigma$ . Note that the most of gamma-ray sources with high galactic latitudes are blazars and that blazars

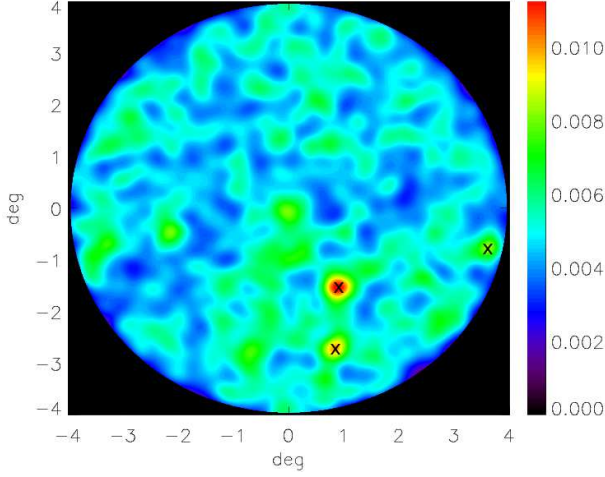


**Fig. 1.** Gaussian ( $\sigma = 0.15^\circ$ ) kernel smoothed count map (before the subtraction of 2FGL sources) centered on the positions of galaxy clusters for the energy range 10 GeV–270 GeV and for a pixel size of  $0.005^\circ \times 0.005^\circ$

are variable gamma-ray sources in time (e.g. Nolan et al. 2012). Flaring activity of blazars can lead to higher TS values (compared with those listed in the 2FGL catalogue) when the 52.5 months of the data are analyzed and, therefore, we mask the 2FGL gamma-ray sources to estimate the background emission around the selected galaxy clusters. The masked 2FGL gamma-ray sources are listed in Table A.1. In this Table, we show the names of 2FGL sources, the square root of the TS values at  $E > 10$  GeV (from the 2FGL catalogue), and the names of galaxy clusters located within a circle of  $4^\circ$  radius around each of the sources. To mask these 2FGL sources, we use a circle with a radius of  $0.5^\circ$ , corresponding to the  $\approx 90\%$  angle containment radius, centered on the positions of these sources. The stacked count map of the selected galaxy clusters obtained by combining the count maps for each of the galaxy clusters from our sample with equal weights and smoothed with a Gaussian kernel ( $\sigma = 0.15^\circ$ ) is shown in Fig. 1 (and Fig. 2) before (and after) the subtraction of 2FGL point sources. Each count map is aligned in galactic coordinates. We do not scale the count maps because the virial radii of the selected galaxy clusters are in a narrow range of  $0.4^\circ$ – $0.65^\circ$ . The crosses in Fig. 1 show the positions of bright 2FGL gamma-ray sources, 2FGLJ0710.5+5908, 2FGLJ1256.1-0547, and 2FGLJ1800.5+7829. Note that the counts of isotropic background emission that subtracted along with the 2FGL point sources do not strongly affect the estimation of isotropic background emission. This is because the total surface area covered by the masked regions is only  $\approx 1.8\%$  of the total surface area covered by the regions of interest around the selected clusters of galaxies.

Figure 2 demonstrates the excess of the number density of counts towards galaxy clusters (i.e., towards the central region of this count map) over the average number density of counts. Studies of spatial, temporal, and spectral properties of the observed tentative signal towards galaxy clusters will be presented below. There are three possible interpretations of this central excess: 1) it is due to gamma-ray emission from galaxy clusters; 2) it is due to a high local concentration of non-2FGL point sources towards galaxy clusters; and 3) it is due to processes occurring in the ICM, but not directly related to galaxy cluster emission. The evaluation of statistical significance of this gamma-ray signal to-

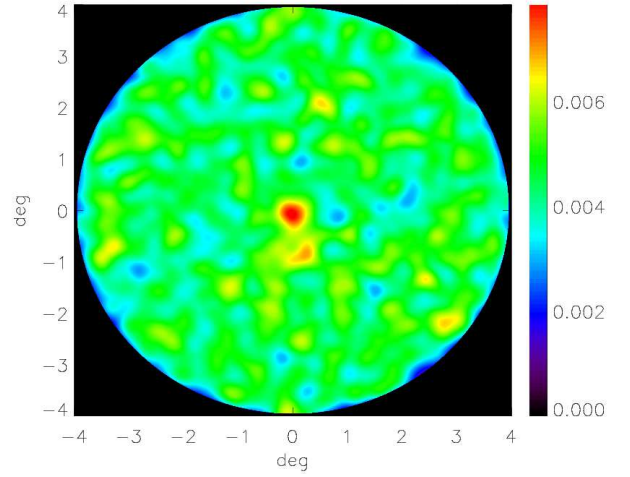


**Fig. 2.** Gaussian ( $\sigma = 0.15^\circ$ ) kernel smoothed count map (after the subtraction of 2FGL sources) centered on the positions of galaxy clusters for the energy range 10 GeV–270 GeV and for a pixel size of  $0.005^\circ \times 0.005^\circ$

wards galaxy clusters and the study of the origin of the central count density excess will be present in the Sect. 3.

### 3. Results

In this Section, we evaluate the statistical significance of the observed gamma-ray signal towards the selected clusters of galaxies and study various interpretations of this signal.

#### 3.1. Evaluation of the significance of the signal

To evaluate the statistical significance of the observed gamma-ray signal towards the selected galaxy clusters, we bin the count map (its smoothed version is shown in Fig. 2), into concentric annuli. We choose the surface area of each of the annuli equal to  $\pi(0.25^\circ)^2$ . This value of surface area corresponds the 68% containment angle at 10 GeV. Thus, the first annulus, which covers the center of the count map, should contain  $\approx 68\%$  of gamma-rays incoming from these galaxy clusters if the signal is strongly centrally concentrated. The radius of the  $k$ -th annulus is given by  $R_k = \sqrt{k} \times 0.25^\circ$ . Note that the widths of annuli strongly decrease with radius, but this does not affect an estimate of isotropic background emission. The numbers of photon events in the first twenty annuli (starting from the center of the count map) are shown in Fig. 3. These twenty annuli cover the circular region with a radius of  $\approx 1.1^\circ$ . The radial distribution of photons, shown in Fig. 3, confirms the presence of a high count density in the center of the count map. The number of counts in the first annulus equals 63 and is significantly higher than the numbers of counts in other radial bins.

The expected number of photons from background emission should be estimated in order to calculate the significance level of the observed central gamma-ray excess. Since the selected galaxy clusters are at high galactic latitudes ( $|b| > 20^\circ$ ), the background emission can thus be considered as isotropic. We calculate the expected number of background photons in the first annulus. First, we estimate the expected number of background photons using the nineteen outer annuli. The mean value of photons within an annulus is 37.1 and the standard deviation equals 5.2. Second, we calculate the expected number of background photons taking the regions of  $4^\circ$  radius and excluding their most

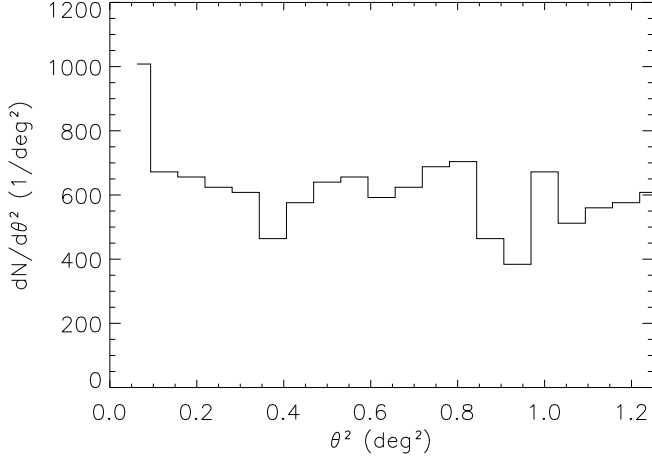


**Fig. 3.** Radial distribution of photons in annuli with surface area of  $\pi(0.25^\circ)^2$

central parts of  $0.25^\circ$ . By means of the second method, we found that the mean value of background photons within an annulus is 36.7 and is in good agreement with that calculated by using the first nineteen annuli. Therefore, the observed number of counts within the first annulus equal to 63 is significantly higher than the expected number of background counts, i.e. 36.7. The statistical significance level of the count density excess in the first annulus over the expected value equals  $(63 - 36.7) / \sqrt{36.7} \approx 4.3\sigma$ .

We perform the spatial analysis of the central gamma-ray excess to check if the radial distribution of counts agrees with that of a point source or of an extended source. Note that the mean virial radius of the selected galaxy clusters corresponds to  $\approx 0.5^\circ$  and, therefore, if the observed excess is produced due to emission via neutral pion decay then this signal should be modestly extended and its maximal brightness should be at the center. Assuming that the gamma-ray brightness profiles follow those for X-ray brightness derived from a beta model and taking the values of the parameters for a beta model for the selected galaxy clusters from the HIFLUGCS catalogue (Reiprich & Böhringer 2002), we found that the 68% gamma-ray emission from these clusters should be confined within the central region with a radius of  $0.25^\circ$ . The possible IC gamma-ray emission from the structure formation shocks around galaxy clusters should have an extended profile with maximal brightness at shock fronts. However, if gamma-ray emission from galaxy clusters comes from AGNs located in the most central regions of galaxy clusters (such as NGC 1275 in center of the Perseus cluster (Abdo et al. 2009)), the observed radial distribution of counts should be described as a point source. For studying the spatial extension of the observed signal towards galaxy clusters, we use three models (a point source for emission from central AGNs, a disk model for emission produced via neutral pion decay, and a thick ring model for emission produced via the IC radiation from structure formation shocks). To perform the spatial analysis, we bin the count map into concentric annuli with surface area of  $\pi \times (0.25^\circ)^2 / 2$ . The numbers of observed counts in the first sixteen annuli from the center are 33, 30, 30, 13, 19, 21, 20, 22, 20, 16, 16, 11, 19, 16, 20, and 18. The outer radius of the sixteenth bin is  $1^\circ$  and corresponds to  $\approx 2R_{\text{vir}}$ .

We produce six spatial templates to estimate the significance level of the observed gamma-ray excess. The first template map describes a point-like source and is obtained by the convolu-

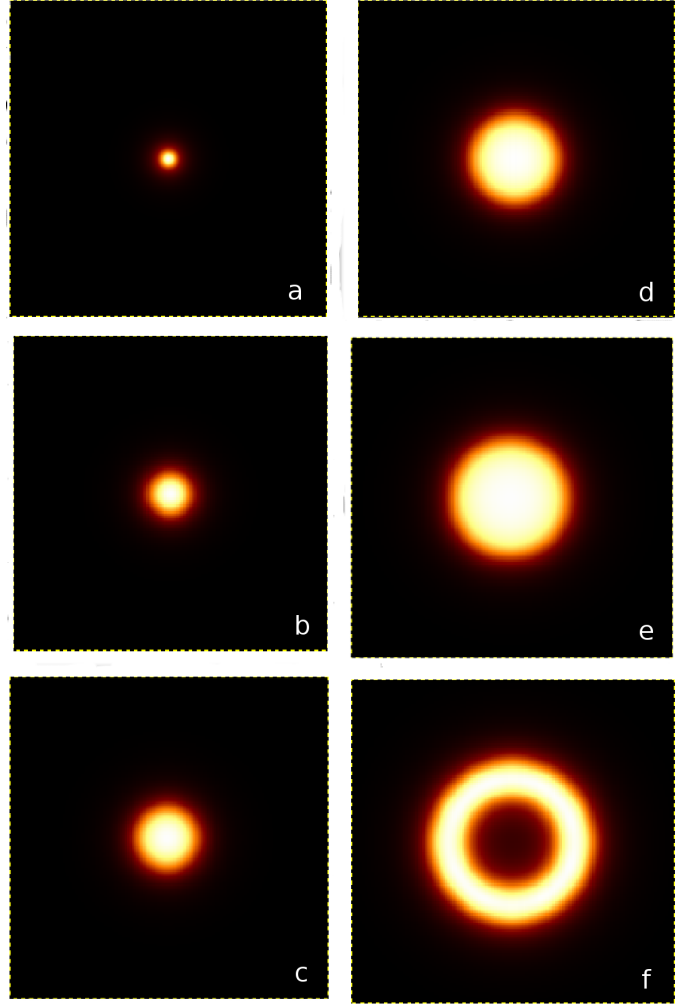


**Fig. 4.** Two dimensional templates (with a size of  $3 \times 3 \text{ deg}^2$ ) for the gamma-ray emission from galaxy clusters: (a) a point source template; (b-e) templates for emission from a disk of radius  $0.15^\circ$ ,  $0.25^\circ$ ,  $0.375^\circ$ , and  $0.5^\circ$ ; (f) a ring-like spatial template

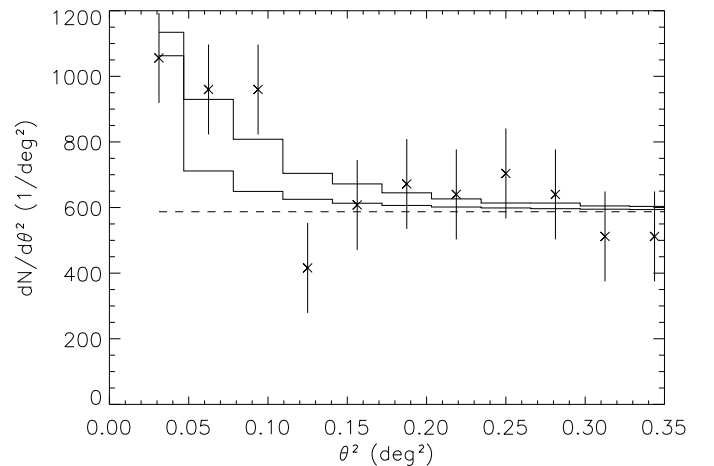


**Fig. 5.** The best fits of the point source and disk ( $R=0.25^\circ$ ) source models to the data shown by thin and thick solid lines, respectively. The surface area of a annular bin is  $\pi(0.25^\circ)^2/2$ .

**Table 1.** The significance of signal detection

Template	Convolution with the PSF	Significance
disk (R=0.25°)	no	4.3σ
point source	yes	4.1σ
disk (R=0.15°)	yes	4.6σ
disk (R=0.25°)	yes	4.7σ
disk (R=0.375°)	yes	4.2σ
disk (R=0.5°)	yes	3.5σ
ring (0.45° <R< 0.65°)	yes	<1σ

tion of a point source model with the PSF. The following four template maps describe the count distributions for extended disk sources with radii of 0.15°, 0.25°, 0.375°, and 0.5° and correspond to the possible neutral pion decay emission from galaxy clusters. The sixth template map describes an extended ring-like profile with inner and outer radii of 0.45° and 0.65° (corresponding to  $\approx 0.9 R_{\text{vir}}$  and  $\approx 1.3 R_{\text{vir}}$ ), respectively, and corresponds to the possible IC emission from the structure formation shocks around galaxy clusters. All the disk-like and ring-like spatial templates are convolved with the PSF. To calculate the PSF, we adopt the power-law spectral distribution for each template with a photon index of  $-2.1$ . The produced templates are shown in Fig. 4. To calculate the number of counts,  $N_{\text{src}}$ , observed from the gamma-ray source with one of the spatial profiles, shown in Fig. 4, we use the equation

$$N_{\text{src}} = \frac{\sum_{k=1}^{16} N_k p_k}{\sum_{k=1}^{16} p_k^2}, \quad (4)$$

where  $p_i$  are weights for each of the annuli determined by the spatial profile for a source model and  $N_k$  is the number of observed counts in the  $k$ -th annulus minus the number of counts from isotropic background. The best fits of the point source and disk source (with a radius of 0.25°) models to the data are shown in Fig. 5 by thin and thick solid lines. The expected number of counts from isotropic background is shown in Fig. 5 by a dashed line. The number of observed counts in each annular bin along with the errorbars is also plotted in this Figure. Using the number of counts observed from the source for each of the models, we calculate the significance level of the observed gamma-ray excess. The calculated value of the significance level is  $4.1\sigma$  for the point source template. The values of the significance level are  $4.6\sigma$ ,  $4.7\sigma$ ,  $4.2\sigma$ , and  $3.5\sigma$  for the templates describing gamma-ray emission from disks with radii of 0.15°, 0.25°, 0.375°, and 0.5°, respectively. As for the ring-like model, we found no evidence for the IC emission around galaxy clusters and that the observed numbers of counts in outer annuli agree with that expected from background emission within  $1\sigma$ . Thus, the model for gamma-ray emission from structure formation shocks cannot account for the observed gamma-ray excess towards the selected galaxy clusters. We list the significance levels for our spectral-spatial templates in Table 1.

We use the sample of 55 galaxy clusters and bin the observed counts in annuli as described above to calculate the Poisson log-likelihood for each of the spectral-spatial models listed in Table 1. Fitting a disk model to the data improves the log-likelihood by  $\Delta L \approx 2.5$  in comparison to the point-source hypothesis. This provides evidence of the spatial extension of the gamma-ray source at a significance level of  $\sqrt{2} \times \Delta L \approx 2.2\sigma$ . Note that this significance level is not sufficient to claim that the gamma-ray source in the directions of galaxy clusters is extended.

We conclude that the significance level of the central gamma-ray excess is greater than  $4\sigma$  for several spatial models, such as a point-like source model and a disk-like source model.

### 3.2. The individual contributions of galaxy clusters to the observed gamma-ray signal

In this Section, we estimate the contribution of each galaxy cluster to the total observed gamma-ray signal towards the selected galaxy clusters and check the consistency of the observed distribution of the number of photon events in galaxy clusters with a Poisson distribution. We also test homogeneity of incoming photons in time to check if the observed gamma-ray signal towards galaxy clusters can be explained by time-invariant mechanisms of gamma-ray production, such as those via neutral pion decay or via the IC effect.

#### 3.2.1. Distribution of the number of photon events in galaxy clusters

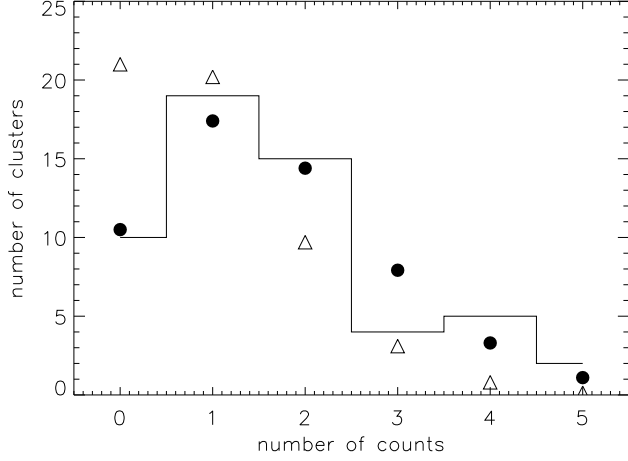
To study the origin of the observed signal towards the selected clusters of galaxies, we perform an analysis of the distribution of counts in galaxy clusters. Note that the first three annular bins, shown in Fig. 5, provide us with the highest signal-to-noise ratio of  $(93 - 36.7 \times 1.5) / \sqrt{36.7 \times 1.5} \approx 5.1$ . Thus, for this study we select counts in the directions of the clusters from our sample within a circle of 0.3° radius. Below, we calculate the expected number of galaxy clusters with a given number of counts within a circle of 0.3° radius and compare the expected and observed numbers of galaxy clusters.

The total number of counts in the directions of the galaxy clusters within a circle of 0.3° radius equals 91. Therefore, the average number of counts incoming from the direction of a cluster is given by  $91/55 \approx 1.65$ . Assuming the Poisson distribution, we calculate the probability to detect a given number of counts towards a galaxy cluster. As expected, the most of the circular regions ( $\approx 75\%$ ) contains 0, 1, and 2 counts. The expected numbers of clusters with 0–6 counts within a circular region of 0.3° radius are shown in Table 2. If the observed gamma-ray excess towards the selected galaxy clusters is due to one or two strong gamma-ray sources then the number of circular regions with a high number of counts should be significantly higher than that obtained from an estimate based on the Poisson distribution. We calculate the observed numbers of clusters with 0–6 counts within a circular region of 0.3° and list the observed numbers of counts in Table 2. We find that there is no circular region with a radius of 0.3° containing more than five counts. The difference of the observed number of circular regions with the number of counts,  $> 2$ , and the expected number of such regions obtained from the Poisson distribution with parameter  $\lambda = 1.65$  is  $\approx -2$ . We conclude that the observed number of circular regions with a number of counts higher than 2 towards the galaxy clusters is consistent with that obtained from the Poisson distribution with parameter  $\lambda = 1.65$ . Therefore, the contribution of one or two possible strong gamma-ray sources to the observed gamma-ray excess cannot explain the observed excess.

We also calculate the number of circular regions with a given number of counts that expected from the background emission. The average number of counts within a circular region of 0.3° radius coming from background emission is  $52.8/55 \approx 0.96$ . The difference of the observed number of circular regions with the number of counts,  $> 2$ , and the number of such regions expected from background diffuse emission equals  $\approx 29$  counts (i.e.,

**Table 2.** The expected and observed numbers of galaxy clusters with a given number of counts

Numbers of counts	Expected number of clusters	Observed number of clusters
0	10.5	10
1	17.4	19
2	14.4	15
3	7.9	4
4	3.3	5
5	1.1	2
6	0.3	0


**Fig. 6.** The observed number of galaxy clusters with a given number of counts (histogram) and the expected numbers from the Poisson distribution with  $\lambda = 1.65$  (filled circles) and with  $\lambda = 0.95$  (open triangles)

$\approx 55\%$  of the photons expected from the background emission). We recalculate the significance of detection of a gamma-ray signal towards the selected galaxy clusters excluding the eleven galaxy clusters with the highest observed number of counts within a central circular region of  $0.3^\circ$  radius and found that the detection significance of the excess decreases from  $\approx 4.7\sigma$  to  $1.5\sigma$ . Therefore, the analysis of these eleven galaxy clusters is important to understand the origin of the observed gamma-ray excess. In Fig. 6 we plot the observed and expected distributions of the numbers of galaxy clusters with a given number of counts.

Note that the probability to observe a given number of counts by chance varies from one galaxy cluster to another galaxy cluster and depends on the expected number of counts from background around each cluster of galaxy. We calculate the expected number of background counts for each of the eleven galaxy clusters with the highest observed number of counts. To calculate the number of background counts for each circular region with a radius of  $4''$ , we mask 2FGL sources. The calculated numbers of background counts are shown in Table 3 for these eleven galaxy clusters. Using the Poisson statistics, we calculate the probability to obtain the observed number of counts by chance. The obtained probabilities are listed in the fourth column in Table 3. Note that the probability to observe 4 or 5 counts in a circular region of  $0.3^\circ$  radius by chance is less than 3%.

**Table 3.** Probability to obtain the observed number of counts from background emission by chance

Cluster name	Observed counts	Background	Probability, %
A0119	3	0.73	3.1
A3112	3	0.72	3.0
A4038	3	0.73	3.1
ZwIII54	3	1.33	10.4
A0400	4	1.05	1.8
2A0335	4	1.20	2.6
A1367	4	0.85	0.9
MKW4	4	0.73	0.6
A2255	4	1.16	2.4
A2063	5	0.86	0.2
A3581	5	1.04	0.4

### 3.2.2. Test for homogeneity of incoming photons in time

Gamma-ray emission from galaxy clusters produced via neutral pion decay and via the IC emission does not vary with time within the time-range of an observation. We use this argument to check if the observed gamma rays with  $E > 10$  GeV towards the selected galaxy clusters are homogeneously distributed in time. To perform the test, we choose the galaxy clusters with a high number of observed counts in their directions listed in Table 3. In Table A.2 we list the arrival time, given in the Mission Elapse Time (MET) units, and the energy for each photons within a circular region of  $0.3^\circ$  radius centered on A0119, A3112, A4038, A0400, 2A0335, A1367, MKW4, A2255, A2063, and A3581. Note that we withdraw ZwIII54 from the sample shown in Table 3, because the probability, 10.4%, to obtain the observed number of counts from background emission by chance for this galaxy cluster is significantly higher than that for other galaxy clusters from Table 3. We use the nearest-neighbor method for testing the homogeneity hypothesis and calculate the sum of the distances between each event and its nearest neighbor in time. This provides a test statistic that requires no partitioning scheme. Note that the observed number of counts in a short time interval depends on exposure duration. The exposure duration for successive intervals of time corresponding to the precession period of the orbit of the *Fermi* spacecraft,  $\approx 55$  days, is roughly constant. Since we use the 52.5 months of the data, the observation time contains  $\approx 28$  time intervals of almost equal exposure. Performing the Monte-Carlo simulations for the homogeneous distribution of counts in time, we calculate the number of simulation runs with the statistic value less than that calculated for each galaxy cluster from Table 3. The obtained number of simulation runs with the statistic value less than that for A0199 is 12% of the simulations, A3112 - 6%, A4038 - 77%, A0400 - 54%, 2A0335 - 48%, A1367 - 60%, MKW4 - 57%, A2255 - 17%, A2063 - 8%, and A3581 - 17%. We also perform a more powerful test for homogeneity by calculating the probability of several independent simulation runs with a given number of simulated counts to obtain the test statistic value in each simulation run lower than that is derived from the observation of one of the galaxy clusters having the number of counts in its direction the same as that simulated. The probability that one of three independent Monte-Carlo simulation runs with the homogeneous distribution of 3 photons in time gives the statistic value less than that for A0199, and two other simulation runs give the statistic values less than those for A3112 and A4038 equals 2.2%. The probability that one of five independent Monte-Carlo simulation runs with the homogeneous distribution of 4 photons in time gives the statistic value less than that for A0400, and four other simulation

runs give the statistic values less than those for 2A0335, A1367, MKW4, and A2255 is less than 6.3%. The probability that one of two independent Monte-Carlo simulation runs with the homogeneous distribution of 5 photons in time gives the statistic value less than that for A2063, and the other simulation run gives the statistic value less than that for A3581 equals 2.0%. We conclude that the observed gamma rays are not homogeneously distributed in time and that the observed gamma-ray excess towards the selected galaxy clusters cannot be totally produced by the emission via neutral pion decay and by the IC emission. Before starting the search for time variable gamma-ray sources in the directions of the selected galaxy clusters, we note that different sky-survey profiles have been used on Fermi and, therefore, the on-source exposure also varies in time because of the use of different sky-survey profiles. We do not include the exposure variation due to the sky-survey profiles in the present analysis and assume that this effect does not affect the result presented in this Section. In Sect. 3.3, we study the catalogue of AGNs to search of time variable gamma-ray sources towards the selected galaxy clusters.

### 3.3. Time variable sources towards galaxy clusters

Many of the high-latitude 2FGL gamma-ray sources are associated with the bright, flat radio spectrum active galactic nuclei (AGNs) known as blazars. A uniform all-sky Candidate Gamma-Ray Blazar Survey (CGRaBS) selected primarily by flat radio spectra was performed by Healey et al. (2008) to provide a large catalogue of likely gamma-ray AGNs suitable for identification of high-latitude gamma-ray sources detected with *Fermi*-LAT. The CGRaBS catalogue contains 1625 gamma-ray candidate sources with radio and X-ray properties similar to those of the EGRET blazars, spread uniformly across the  $|b| > 10^\circ$  sky. 81% of these gamma-ray candidate sources have measured redshifts. Identification of a fraction of gamma-ray sources towards the 55 selected galaxy clusters with blazars will allow us to focus on the gamma-rays incoming from galaxy clusters. Note that not all detected blazars by *Fermi*-LAT are included in the CGRaBS catalogue and that  $>1000$  sources from the CGRaBS catalogue have not yet been detected by *Fermi*-LAT.

We perform the search of gamma-ray candidate sources from the CGRaBS catalogue within a circle of  $0.6^\circ$  (which slightly exceeds the mean virial radius and the 2 PSF) towards the selected galaxy clusters and found that the gamma-ray candidate sources are present towards eight galaxy clusters, namely A0400, A3395s, A3558, A3581, A2029, A2147, A2634, and A2637. The distances between each of these galaxy clusters and its nearest gamma-ray source candidate from the CGRaBS catalogue is 26.6' for A0400, 9.9' for A3395s, 20.2' for A3558, 30.8' for A3581, 28.8' for A2029, 20.2' for A2147, 33.3' for A2634, and 31.3' for A2657. We list the redshifts of these galaxy clusters and of the nearest gamma-ray CGRaBS source for each of these clusters, and the number of counts within a circle of  $0.3^\circ$  radius around each of these galaxy clusters in Table 4. This Table shows that six of these eight blazars have redshifts larger than 0.35. Note that two of these galaxy clusters, namely A0400 and A3581, are also present in Table 3. The associated CGRaBS gamma-ray candidate sources with A0400 and A3581 are very distant and have redshifts of 1.381 and 2.43, respectively.

We calculated the number of CGRaBS candidate gamma-ray sources within the first sixteen annuli with surface of  $\pi(0.6^\circ)^2$  centered on the 55 selected galaxy clusters and found that the first inner annulus contains 8 CGRaBS sources while the mean value of CGRaBS sources within an annulus is 2.8. Thus, the probability of the presence of 8 CGRaBS sources within the in-

**Table 4.** List of galaxy clusters possibly contaminated by CGRaBS sources, located at the projected distance  $<0.6^\circ$  from the cluster centers

Cluster name	Number of counts	Redshift of a clusters	Redshift of a blazar	Max. energy (GeV)
A0400	4	0.024	1.381	50.8
A3395s	1	0.0498	2.051	43.5
A3558	1	0.048	1.326	19.7
A3581	5	0.0214	2.43	16.8
A2029	2	0.0767	0.084	21.4
A2147	0	0.0351	0.109	–
A2634	1	0.0312	0.372	15.1
A2657	2	0.0404	0.667	24.4

nerest annulus is only  $\approx 0.57\%$ . We also calculated the number of CGRaBS candidate gamma-ray sources within the first sixteen annuli with surface of  $\pi(0.5^\circ)^2$  (the radius of the first annulus corresponds to the mean virial radius of the 55 selected clusters) and found each of the first two annuli contains 4 CGRaBS sources. The probability of the presence of 4 CGRaBS sources within such an annulus is only  $\approx 1.4\%$ . We conclude that the number of CGRaBS gamma-ray candidate sources towards the selected galaxy clusters exceeds the expected number within the central annulus with a radius of  $0.5^\circ$  (and  $0.6^\circ$ ). One of the possible explanations of the high concentration of CGRaBS sources towards these galaxy clusters is a statistical deviation from the expectation.

Note that high-energy gamma-rays interact with long-wavelength photons of the extragalactic background light producing electron-positron pairs (the Breit-Wheeler process), see, e.g., Kneiske et al. (2002); Franceschini et al. (2008); Finke et al. (2010). The absorption of gamma-rays from distant sources, such as blazars, via  $e^-e^+$  pair creation leads to decrease the observed flux at high energies,  $E_\gamma > 20$  GeV (e.g., Finke et al. 2010). We use the absorption optical depth of gamma-ray photons as a function of observed gamma-ray photon energy, calculated by Finke et al. (2010), to test the possibility to observe high energy photons from the distant CGRaBS sources at  $z=1.381$ ,  $2.051$ ,  $1.326$ , and  $2.43$ , towards A0400, A3395s, A3558, and A3581, respectively. We list the maximal observed energy of photons towards these galaxy clusters in Table 4. We take the values of absorption optical depth from the tables<sup>2</sup>. The absorption optical depth for a gamma-ray with observed energy of 50.8 GeV emitted at  $z=1.38$  is  $\approx 0.57$ , for a gamma-ray with observed energy of 43.5 GeV emitted at  $z=2.05$  is  $\approx 0.77$ , for a gamma-ray with observed energy of 19.7 GeV emitted at  $z=1.33$  is  $\approx 0.022$ , and for a gamma-ray with observed energy of 16.8 GeV emitted at  $z=2.43$  is  $\approx 0.1$ . We calculated the probability of detection of high energy gamma-rays towards these CGRaBS sources in the framework of the absorption model of gamma-rays on the extragalactic background light and found that the detection of the highest energy gamma-rays towards the most of these CGRaBS sources is consistent with the expectation from the absorption model. However, the probability of detection of a 43.5 GeV photon towards A3395s without observing any photons with energies between 10 GeV and 43.5 GeV towards this cluster is only 0.25% and, therefore, it is hardly possible that the detected 43.3 GeV photon was emitted by a distant blazar.

<sup>2</sup> <http://www.phy.ohiou.edu/~finke/EBL/>

### 3.4. Likelihood analysis of gamma-ray emission in the directions of A0400 and A3581

We perform a binned likelihood analysis of gamma-ray emission at the positions of the Abell 400 (A0400) and Abell 3581 (A3581) galaxy clusters. These two clusters are selected for an analysis because of their presence both in Table 3 of clusters with the largest number of events at  $E > 10$  GeV and in Table 4 of clusters possibly contaminated by CGRaBS candidate gamma-ray sources. The presence of possible gamma-ray sources, namely a binary black hole system 3C 75 in A0400 and a blazar PKS 1404-267 in A3581, also provides a good reason for a search of gamma-ray emission from these galaxy clusters. The test statistic (TS) is employed to evaluate the significance of the gamma-ray fluxes coming from these two galaxy clusters. The TS value is used to assess the goodness of fit and is defined as twice the difference between the log-likelihood functions maximized by adjusting all parameters of the model, with and without the source, and under the assumption of a precise knowledge of the galactic and extragalactic diffuse emission. We use the publicly available tool (*glike*), released by the *Fermi*-LAT collaboration, to perform a binned likelihood analysis. For each analyzed source, we select events with energy  $E > 100$  MeV in a circular region of interest of  $20^\circ$  radius. We use the first 52.5 months of the *Fermi*-LAT data and the good time intervals such that the region of interest does not go below the Earth Limb. We use the spectral-spatial templates, *gal\_2yearp7v6\_v0.fits* and *iso-p7v6source.txt*, for the galactic and extragalactic diffuse emission, respectively. To produce a spectral-spatial model for each galaxy cluster, we fix their positions at the localization of 3C 75 for A0400 and of PKS 1404-267 in A3581 and include the gamma-ray sources from the 2FGL catalogue. The spectra of 2FGL sources are taken from the 2FGL catalogue. The spectral parameters of the most of 2FGL sources are fixed at the 2FGL values, while the parameters of the strongest sources in the region of interest are left free in the likelihood fit. We model the emission from these two galaxy clusters under the assumption of a point source with a power-law spectral distribution. The likelihood ratio test shows that the TS values for A0400 and A3581 equal 41.7 and 5.3, respectively. The approximate value of the significance of detection is given by  $\sqrt{TS}\sigma$  and, therefore, the significance of detection is  $6.4\sigma$  and  $2.3\sigma$  for A0400 and A3581, respectively. Note that the possible explanation of a higher significance value for A400 is that diffuse emission is strongly inhomogeneous on a scale of  $\approx 5^\circ$  towards this galaxy cluster. The performed likelihood analysis shows that the gamma-ray sources towards these galaxy clusters will be promising targets for an analysis in the future.

### 3.5. Cool-core and non-cool core galaxy clusters

Clusters of galaxies with dense gaseous cores have central cooling times much shorter than a Hubble time. XMM-Newton observations of cool-core galaxy clusters have shown that the spectral features predicted by the cooling flow models are absent in the X-ray spectra (Peterson et al. 2001, 2003). The likely source of energy, compensating gas cooling losses, comes from central AGN (e.g., Churazov et al. 2000; David et al. 2001; Böhringer et al. 2002). The presence of dense gaseous cores in cool-core clusters can lead to the increase of gamma-ray emission due to neutral pion decay produced in the collisions of relativistic protons with protons of the ICM, while the central AGN itself can also be a source of gamma-ray emission. Non-cool core clusters in their turn often show evidence of a merger

**Table 5.** The significance of signal detection for the samples of cooling core and non-cooling core galaxy clusters

Template	cooling core clusters	non-cooling core clusters
point source	$4.3\sigma$	$1.8\sigma$
disk ( $R=0.15^\circ$ )	$4.9\sigma$	$2.0\sigma$
disk ( $R=0.25^\circ$ )	$5.0\sigma$	$2.0\sigma$
disk ( $R=0.375^\circ$ )	$4.6\sigma$	$1.8\sigma$
disk ( $R=0.5^\circ$ )	$3.5\sigma$	$1.9\sigma$

and, therefore, CR hadrons and electrons accelerated in merger shocks can lead to gamma-ray emission via the neutral pion decay or IC effect. In this Sect., we perform an analysis of a sample of cool-core galaxy clusters and of a sample of non-cool core clusters to study gamma-ray emission of these two distinct types of galaxy clusters.

We divide 55 selected galaxy clusters into the two samples using the definition from Chen et al. (2007). If the ratio of the mass deposition rate,  $\dot{M}$ , to the cluster mass,  $M_{500}$ , for a galaxy cluster exceeds  $10^{-13} \text{ yr}^{-1}$  then the galaxy cluster belongs to the sample of cool-core clusters. The second sample of galaxy clusters consists of galaxy clusters with the ratio,  $\dot{M}/M_{500}$ , smaller than  $10^{-13} \text{ yr}^{-1}$ . We take the values of  $\dot{M}/M_{500}$  and  $M_{500}$  from Tables 1 and 4 of Chen et al. (2007). There are two galaxy clusters, A1651 and A2063, with the calculated ratios of  $\dot{M}/M_{500}$  close to  $10^{-13} \text{ yr}^{-1}$ . We include these two clusters in the sample of cool-core clusters. The sample of cool-core clusters consists of 27 clusters and the sample of non-cool core clusters consists of 28 clusters.

Using the spectral-spatial templates presented above, we calculate the significance of detection of a gamma-ray signal from both the samples. The method used to evaluate the statistical significance is analogous to that applied in Sect. 3.1. The evaluated values of the significance of detection are shown in Table 5. We found that the significance of the gamma-ray signal from the sample of cool-core clusters,  $\approx 5\sigma$ , is significantly higher than that from the sample of non-cool core clusters  $\approx 2\sigma$ . Furthermore, we conclude that the observed excess of gamma-ray emission in the direction of the 55 selected clusters is mainly owing to gamma rays coming from the cooling core clusters.

Assuming that the numbers of observed photons in both the samples of galaxy clusters can be modeled by a Poisson distribution, we check if the two Poisson samples have the same mean. To perform this analysis, we use the test-statistics,  $TS = (O_1 - E_1)^2/E_1 + (O_2 - E_2)^2/E_2$ , where  $O_{1,2}$  are the observed number of photons within a circle of  $0.3^\circ$  centered on galaxy clusters from each sample and  $E_{1,2}$  is the number of photons expected under the assumption that the two Poisson samples have the same mean. We found that the probability that both the samples have the same mean is 6.3%. We conclude that the contribution of cooling-core clusters to the gamma-ray emission from the 55 selected clusters is dominant over that of non-cooling core clusters. Therefore, the gamma-ray properties of the cooling core clusters significantly differs from those of the non-cooling core clusters.

Note that our selection of 55 galaxy clusters is based on the flux limited cluster sample from the HIFGLUGS catalogue. Therefore, the expected proportionality between X-ray and neutral pion decay induced gamma-ray fluxes (see Ensslin et al. 1997) leads to a testable prediction about higher gamma-ray fluxes from brighter X-ray galaxy clusters. Taking this prediction into account, we perform a likelihood analysis weighting the observed number of gamma rays from each galaxy cluster with its expected gamma-ray flux. We calculate the Poisson

loglikelihood for each of the spectral-spatial models using two weighting techniques: 1) combining the observed count maps with equal weights (as was done in Sect. 3.1) and 2) weighting the observed number of counts with expected gamma-ray fluxes. We compute the difference in the maximized values of the log-likelihood (L) functions for both weighting techniques and for each spectral-spatial model and found that the maximal likelihood for the “equal weights” model is larger than that for the hadronic model of gamma-emission. We use the Akaike information criterion to measure the relative quality of the models supporting these two weighting techniques and found that the hadronic model of gamma-emission is  $\exp(L_2 - L_1) \approx 5 \times 10^{-3}$  times as probable as the “equal weights” model to minimize the information loss. The significance of detection of a signal in the direction of the 55 selected galaxy clusters is in the range of  $2.1\text{-}2.7\sigma$  (depending on the spectral-spatial models) when the weighting technique presuming the expected gamma-ray fluxes from the hadronic model is used. Therefore, there is no convincing evidence that observed signal is due to neutral pion decay, at least in the simplest version of the model presuming  $F_\gamma \propto F_X$ .

### 3.6. Upper limit on relativistic-hadron-to-thermal energy density ratio

We reevaluate the significance of a gamma-ray signal from clusters of galaxies withdrawing 8 galaxy clusters possibly contaminated by CGRaBS gamma-ray candidate sources (see Sect. 3.3) from our sample. Using the method described in Sect. 3.1 and the templates for gamma-ray emission produced above, we found that the values of the significance level are  $3.3\sigma$ ,  $3.6\sigma$ ,  $3.2\sigma$ , and  $2.3\sigma$  for the disk templates with radii of  $0.15^\circ$ ,  $0.25^\circ$ ,  $0.375^\circ$ , and  $0.5^\circ$ , respectively. The significance level for the point source template is  $2.7\sigma$ . For the ring-like model, we found no evidence for an excess over background. Note that the mean number of counts within a circle with a radius of  $0.3^\circ$  centered on the galaxy clusters possibly associated with CGRaBS sources is  $2.0 \pm 0.5$ , while the corresponding average number calculated for the 47 selected galaxy clusters (excluding those that have the possible association with CGRaBS sources) is  $1.6 \pm 0.18$ . For comparison, the mean background contribution to the same region is  $\approx 0.96$  per cluster. A slightly lower flux in the reduced sample is yet another reason (apart from smaller sample size) why the detection significance is lower in the reduced sample.

The energy density stored in hadronic cosmic rays (CR) relative to the thermal energy density of the ICM gas can be constrained by using the observed gamma-ray and X-ray fluxes from galaxy clusters (Ensslin et al. 1997; Ackermann et al. 2010a). Using the Fermi Science Tools<sup>1</sup>, we calculate the exposure weighted by the power-law with a photon index of  $-2.1$  for each of the 47 galaxy clusters to convert count numbers to gamma-ray fluxes at  $E > 10$  GeV. We take the X-ray fluxes from these galaxy clusters and their plasma temperatures from the catalogues published by David et al. (1993); Reiprich & Böhringer (2002). We take the production rate of gamma-rays from Drury et al. (1994) for a spectral index,  $s=4.1$ , of the parent CR hadron distribution  $f(p) \propto p^{-s}$ , where  $p$  is momentum, and extrapolate the production rate at  $E > 1$  TeV to  $E > 10$  GeV. Note that the production rate of gamma-rays is defined as the gamma-ray emissivity normalized to the CR hadron energy density. Using Eq.(10) from Ensslin et al. (1997) and the calculated production rate of gamma-rays at  $E > 10$  GeV, we obtain the relation between the

observed fluxes of gamma-rays,  $F_\gamma(> 10\text{GeV})$ , and X-rays,  $F_X$ , that is given by

$$\frac{F_\gamma(> 10\text{GeV})}{F_X/\text{erg}} \approx 1.33 \left( \frac{k_B T}{\text{keV}} \right)^{1/2} \alpha, \quad (5)$$

where  $\alpha$  is the scaling ratio between the thermal,  $\epsilon_{\text{th}}$ , and CR hadron energy,  $\epsilon_{\text{CR}}$ , densities,  $\epsilon_{\text{CR}} = \alpha \times \epsilon_{\text{th}}$ . Note that the gamma production rate may be taken to be proportional to the number density of relativistic hadrons (Drury et al. 1994) and that the energy density of relativistic particles only slightly depends on the low energy bound for hard power-law hadron spectra with  $s=4.1$ . It is also noteworthy that soft power-law hadron spectra, e.g.  $s=-4.7$ , produce softer gamma-ray spectra and that the value of CR hadron energy density derived by means of this method depends on the assumed power-law hadron spectra. For softer hadron spectra, the factor of 1.33 in Eq. 5 will be lower (e.g.,  $\approx 0.08$  for  $s=4.7$ ) and the contribution of hadrons of energy below about 1 GeV per nucleon, which do not generate observable gamma rays, to the total energy density will be dominant.

To estimate the scaling ratio,  $\alpha$ , from the observed gamma-ray fluxes in the directions of galaxy clusters, we rewrite Eq. 5 as

$$\alpha \approx \frac{1}{1.33} \frac{F_\gamma(> 10\text{GeV})}{F_X/\text{erg}} \left( \frac{\text{keV}}{k_B T} \right)^{1/2}. \quad (6)$$

Putting the parameters into Eq.6, we calculate the scaling ratio  $\alpha$  for each of the selected galaxy clusters. Assuming that the value of the scaling ratio,  $\alpha$ , is the same in these 47 galaxy cluster, we calculate the weighted mean,  $\alpha_\mu$ , and variance of mean,  $\sigma_\mu^2$ , as  $\alpha_\mu = \sum_k (\alpha_k / \sigma_k^2) / \sum_k (1 / \sigma_k^2)$  and  $\sigma_\mu^2 = 1 / \sum_k (1 / \sigma_k^2)$ , where  $\alpha_k$  are the values of the scale ratio for individual galaxy clusters and  $\sigma_k$  are the uncertainties of  $\alpha_k$  (dominated by the uncertainties in  $F_\gamma$ ). Calculating the weighted mean of the scaling ratio and the variance of the mean, we found that the value of the relativistic-hadron-to-thermal energy density ratio equals  $\approx 1.5\%$ . The assumption that this gamma-ray signal is caused by sources variable in time (AGNs) allows us to put an upper limit on the relativistic-hadron-to-thermal energy density ratio equal 1.5%. The possible relativistic hadron component with energy density of 1.5% of that of the thermal plasma does not violate the constraints obtained by an alternative method by Churazov et al. (2008) and its presence should be tested by a combined analysis of the *Fermi*-LAT observations towards the extended galaxy clusters with high X-ray fluxes, such as Virgo, Perseus, Fornax, Hydra, Coma, and Centaurus. An analysis of these extended galaxy clusters is beyond the scope of our paper and requires a more sophisticated technique to deal with the spatial extension of these nearby X-ray brightest clusters of galaxies.

We also study a gamma-ray flux-cluster-mass scaling relation for CR induced emission and compute a prefactor,  $\beta$ , in the relation proposed by (Pinzke et al. 2011)

$$F_\gamma(> 10\text{GeV}) = \beta \times 10^{43} \left( \frac{1}{4\pi D_L^2} \right) \left( \frac{M_{200}}{10^{15} M_\odot} \right)^{1.34} \text{ ph} \cdot \text{s}^{-1} \text{cm}^{-2}, \quad (7)$$

where the gamma-ray flux is dominated by photons produced via the decaying neutral pions and also includes the IC gamma-ray contribution from shock-accelerated primary electrons as well as secondary electrons created in relativistic hadron-proton interactions. The theoretical estimate for the prefactor,  $\beta$ , equals 1.4 (Pinzke et al. 2011). By analogy with the method used in

calculation of the energy density stored in hadronic cosmic rays relative to the thermal energy density, we rewrite Eq.7 as

$$\beta = \frac{F_{\gamma}(> 10\text{GeV})4\pi D_L^2}{10^{43}} \left( \frac{10^{15} M_{\odot}}{M_{200}} \right)^{1.34} \quad (8)$$

and calculate the value of  $\beta$  for each galaxy cluster, the weighted mean  $\beta_{\mu}$ , and variance of mean. We found that the value of the prefactor,  $\beta$ , equals  $3.5 \pm 1.0$  and is slightly higher than that predicted by Pinzke et al. (2011). Given plausible contribution to the gamma-ray flux from central AGNs, we conclude that observed  $\beta \lesssim 3.5$ .

#### 4. Spectral analysis in four energy bands

In the previous Sects., we presented the analysis of gamma-ray emission towards 55 galaxy clusters at energies greater 10 GeV. The tentative gamma-ray excess towards these galaxy clusters at  $E > 10$  GeV was detected. To validate the presence of this gamma-ray excess, below we perform an analysis of gamma-ray emission towards these galaxy clusters in several energy bands. We choose four energy bands for our spectral analysis, which are 1924-3333 MeV, 3333-5773 MeV, 5773-10000 MeV, and  $> 10$  GeV. Low boundaries of these 4 energy bands are logarithmically spaced and the low energy boundary of the first band is chosen taking into account the high spatial resolution at  $E \geq 2$  GeV sufficient to avoid contamination of a signal from galaxy clusters by gamma rays incoming from 2FGL sources.

We use the point and disk source models, described in Sect. 3.1, to calculate the number of observed photons towards galaxy clusters in the four energy bands 1924-3333 MeV, 3333-5773 MeV, 5773-10000 MeV, and  $> 10$  GeV. To perform the spatial analysis, we bin the count maps into concentric annuli with surface area of  $\pi \times \text{PSF}^2/2$ . The evaluated numbers of photons from the source in the directions of galaxy clusters in each energy band are shown in Table 6. The energy bands are enumerated in increasing order in this table. To calculate the PSF in each energy band, we adopted the power-law spectral distribution for each template with a photon index of 2.1. Table 6 shows that the number of photons in the third energy band, i.e. 5773-10000 MeV, is greater than zero at a statistical level of  $\approx 2.5\sigma$ . Thus, the third and fourth energy bands provide an evidence for the possible gamma-ray signal from galaxy clusters.

We estimate the significance of a gamma-ray signal towards galaxy clusters by use of the likelihood ratio method (e.g., see Li & Ma 1983). In the present problem there is one unknown parameter - the expectation of the number of source photons. Note that the expectation of the number of background photons is derived from outer spatial bins where the number of photons coming from the source is negligible. The statistical hypothesis tested here is no extra source exists and all observed photons are due to background. If the errors are Gaussian, then the likelihood is given by  $\mathcal{L} = \exp(-\chi^2/2)$ , so that minimizing  $\chi^2$  is equivalent to maximizing  $\mathcal{L}$ . The correctness of the estimation procedure follows from the fact that variable  $-2 \ln(\mathcal{L}/\mathcal{L}_{\max})$  is distributed like  $\chi^2$  with one degree of freedom if there is one parameter of the problem (see Wilks 1962, chap. 13.7). We re-evaluate the significance of the gamma-ray excess at energies,  $> 10$  GeV, and confirm the results presented in Table 1 of Sect. 3.1 which obtained by means of an alternative method. We perform a combined likelihood analysis in the four energy bins. We found that the value of the significance level is  $4.8\sigma$  for the point source template and that the values of the significance level are

**Table 6.** The evaluated number of counts from the source in the direction of galaxy clusters in four energy bands

Template	$N_{\text{counts, band1}}$	$N_{\text{counts, band2}}$	$N_{\text{counts, band3}}$	$N_{\text{counts, band4}}$
point source	$37.6 \pm 33.6$	$15.0 \pm 16.8$	$20.3 \pm 7.8$	$27.8 \pm 6.7$
disk (R=0.15°)	$40.4 \pm 34.7$	$17.4 \pm 18.1$	$22.0 \pm 8.4$	$30.9 \pm 8.5$
disk (R=0.25°)	$44.3 \pm 36.1$	$20.7 \pm 19.8$	$24.3 \pm 11.0$	$46.0 \pm 9.7$
disk (R=0.375°)	$53.7 \pm 39.3$	$28.3 \pm 19.8$	$28.2 \pm 11.0$	$51.1 \pm 12.1$
disk (R=0.5°)	$68.5 \pm 43.8$	$38.4 \pm 26.7$	$32.2 \pm 13.0$	$49.5 \pm 14.2$

$5.0\sigma$ ,  $5.1\sigma$ ,  $4.8\sigma$ , and  $4.6\sigma$  for the templates describing gamma-ray emission from disks with radii of  $0.15^\circ$ ,  $0.25^\circ$ ,  $0.375^\circ$ , and  $0.5^\circ$ , respectively. Thus, the inclusion of the three low energy bands to the analysis increases the significance of detection of a tentative gamma-ray excess in the directions of galaxy clusters.

#### 5. Conclusions

Clusters of galaxies are promising targets for gamma-ray telescopes. Gamma-rays can be emitted from the ICM via the decay of neutral pions produced in the inelastic proton-proton collisions or via the IC radiation owing to the interaction of very energetic electrons with CMB photons. Apart from these two radiative processes, gamma-rays can also be emitted by the central active galactic nuclei in galaxy clusters. In this paper, we searched for 10 GeV emission from galaxy clusters using the first 52.5 months of the *Fermi*-LAT data. We performed a combined analysis of the 55 galaxy clusters selected from the HIFLUCGS catalogue such that the virial radius of each selected galaxy cluster does not exceed  $1^\circ$ . We selected the photon events with energies above 10 GeV, incoming from the circular regions with a radius of  $4^\circ$  and centered on these 55 galaxy clusters. The selection of this energy interval is motivated by the high angular resolution of *Fermi*-LAT at these energies that permits us to associate more precisely the observed gamma-rays with those that should come from galaxy clusters.

To evaluate the significance of a gamma-ray signal in the direction of the 55 galaxy clusters, we produced six spectral-spatial templates (see Fig. 4) and fitted the models based on these templates to the observed data. The six models include a point source model, four disk models with radii of  $0.15^\circ$ ,  $0.25^\circ$ ,  $0.375^\circ$ , and  $0.5^\circ$ , and a ring model with inner and outer radii of  $0.45^\circ$  and  $0.65^\circ$ , respectively. We found that the significance of the observed signal exceeds  $4\sigma$  for a point source model and for the three first disk models. The highest evaluated significance is  $4.7\sigma$  and is provided by the model of gamma-ray emission from a disk of  $0.25^\circ$  radius. The inclusion of the three low energy bands (1924-3333 MeV, 3333-5773 MeV, and 5773-10000 MeV) to the analysis increases the significance of detection of a tentative gamma-ray excess in the direction of galaxy clusters from  $4.7\sigma$  to  $5.1\sigma$  for the best-fit model. Fitting a disk model to the data improves the likelihood in comparison to the point-source hypothesis, but do not provide strong evidence for spatial extension of the observed gamma-ray signal towards the clusters. We found no evidence for gamma-ray emission from the structure formation shocks described by the ring model.

We performed an analysis of a sample of cool-core galaxy clusters and of a sample of non-cool core clusters to study gamma-ray emission of these two distinct types of galaxy clusters. To divide the 55 selected galaxy clusters into the two samples, we applied the selection criterion based on the estimated ratio of  $\dot{M}/\dot{M}_{500}$  to our sample of galaxy clusters. The performed analysis shows that the contribution of cool-core clusters to the gamma-ray emission from the 55 selected clusters is dominant

over that of non-cool core clusters and that the gamma-ray properties of the cool-core clusters significantly differs from those of the noncooling core clusters.

To reveal the origin of the observed gamma-ray excess in the direction of the 55 selected galaxy clusters, we studied independently the signals from each of these galaxy clusters. We found that there are 10 galaxy clusters in our sample such that the probability to obtain the observed number of photons from each of these clusters within the circular region with a radius of  $0.3^\circ$  by chance is less than 5%. We searched for time variability of the signals from these 10 galaxy clusters using the nearest-neighbor method for testing homogeneity of incoming photons in time. The analysis of time variability showed that the homogeneity hypothesis is not valid and that a fraction of the observed photons has been emitted by variable gamma-ray sources, such as active galactic nuclei.

We performed the search for gamma-ray candidate sources from the CGRaBS catalogue within a circle of  $0.6^\circ$  ( $\approx 2$  PSF) towards the selected 55 galaxy clusters and found that the gamma-ray candidate sources are present towards eight galaxy clusters. Six of these eight CGRaBS gamma-ray candidate sources are distant blazars with redshifts larger than 0.35. We estimated that the significance of a gamma-ray signal after withdrawal of eight galaxy clusters possibly associated with CGRaBS candidate sources. We found that the significance of gamma-ray detection for this subsample is less than that derived from the sample of 55 galaxy clusters and that the highest significance level ( $3.6\sigma$ ) is also provided by the disk model with a radius of  $0.25^\circ$ . Comparing the observed fluxes with those expected in the neutral pion decay model, we found that the best-fit value of the relativistic-hadron-to-thermal energy density ratio equals  $\approx 1.5\%$  for the spectral index of the parent CR hadron distribution,  $f(p) \propto p^{-s}$ , equal  $s=4.1$ . Given that AGNs are likely contributing to the observed flux this value can be treated as an upper limit on the relativistic-hadron-to-thermal energy density ratio, provided that relativistic and thermal components are mixed.

**Appendix A:**

**References**

Abdo, A. A., Ackermann, M., Ajello, M., et al. 2009, ApJ, 699, 31  
 Abdo, A. A., Ackermann, M., Ajello, M., et al. 2010, Physical Review Letters, 104, 101101  
 Ackermann, M., Ajello, M., Albert, A., et al. 2012a, ApJS, 203, 4  
 Ackermann, M., Ajello, M., Allafort, A., et al. 2010a, ApJ, 717, L71  
 Ackermann, M., Ajello, M., Allafort, A., et al. 2010b, JCAP, 5, 25  
 Ackermann, M., Ajello, M., Atwood, W. B., et al. 2012b, ApJ, 750, 3  
 Ando, S. & Nagai, D. 2012, JCAP, 7, 17  
 Araudo, A. T., Cora, S. A., & Romero, G. E. 2008, MNRAS, 390, 323  
 Atwood, W. B., Abdo, A. A., Ackermann, M., et al. 2009, ApJ, 697, 1071  
 Atwood, W. B. e. a. 2007, Astroparticle Phys., 28, 422  
 Bagchi, J., Durret, F., Neto, G. B. L., & Paul, S. 2006, Science, 314, 791  
 Berezhinsky, V. S., Blasi, P., & Ptuskin, V. S. 1997, ApJ, 487, 529  
 Böhringer, H., Matsushita, K., Churazov, E., Ikebe, Y., & Chen, Y. 2002, A&A, 382, 804  
 Brunetti, G. & Lazarian, A. 2007, MNRAS, 378, 245  
 Chen, Y., Reiprich, T. H., Böhringer, H., Ikebe, Y., & Zhang, Y.-Y. 2007, A&A, 466, 805  
 Churazov, E., Forman, W., Jones, C., & Böhringer, H. 2000, A&A, 356, 788  
 Churazov, E., Forman, W., Vikhlinin, A., et al. 2008, MNRAS, 388, 1062  
 David, L. P., Nulsen, P. E. J., McNamara, B. R., et al. 2001, ApJ, 557, 546  
 David, L. P., Slyz, A., Jones, C., et al. 1993, ApJ, 412, 479  
 Dermer, C. D. 1986, A&A, 157, 223  
 Drury, L. O., Aharonian, F. A., & Voelk, H. J. 1994, A&A, 287, 959  
 Dutton, K. L., White, R. J., Edge, A. C., Hinton, J. A., & Hogan, M. T. 2013, MNRAS, 429, 2069  
 Ensslin, T. A., Biermann, P. L., Kronberg, P. P., & Wu, X.-P. 1997, ApJ, 477, 560

**Table A.1.** The list of the masked point sources

2GL source name	$\sqrt{TS}$ at $E > 10$ GeV	cluster name
2FGLJ0009.9-3206	1.7	A4059
2FGLJ0050.6-0929	7.7	A0085
2FGLJ0051.0-0648	2.5	A0085
2FGLJ0055.0-2454	1.4	A0133
2FGLJ0056.8-2111	3.5	A0133
2FGLJ0059.2-0151	4.7	A0119
2FGLJ0118.8-2142	4.0	A0133
2FGLJ0112.8+3208	3.5	NGC507
2 2FGLJ0122.6+3425	5.8	NGC507
2FGLJ0309.1+1027	4.6	A0399, A0401
2FGLJ0325.1-5635	2.1	A3158
2FGLJ0335.3-4501	5.7	A3112
2FGLJ0338.2+1306	5.0	2A0335, ZwIII 54
2FGLJ0414.9-0855	3.8	EXO0422
2FGLJ0416.8+0105	3.4	NGC1550
2FGLJ0423.2-0120	9.0	NGC1550
2FGLJ0424.7+0034	3.4	NGC1550
2FGLJ0647.7-5132	4.0	A3391
2FGLJ0710.5+5908	10.1	A0576
2FGLJ0742.6+5442	—	A0576
2FGLJ0856.6-1105	6.0	A0754
2FGLJ0906.2-0906	3.1	A0754
2FGLJ1141.9+1550	4.2	A1367
2FGLJ1154.0-0010	7.1	MKW4
2FGLJ1229.1+0202	4.7	ZwCl1215
2FGLJ1256.1-0547	16.0	A1650, A1651
2FGLJ1310.9+0036	5.5	A1650
2FGLJ1313.0-0425	—	A1651
2FGLJ1315.9-3339	4.0	A3558
2FGLJ1345.8-3356	1.8	A3562
2FGLJ1347.0-2956	4.2	A3562, A3571
2FGLJ1351.1-2749	1.3	A3581
2FGLJ1406.2-2510	5.1	A3581
2FGLJ1416.3-2415	4.5	A3581
2FGLJ1440.9+0611	6.1	MKW8
2FGLJ1505.1+0324	—	A2029
2FGLJ1506.6+0806	3.2	A2029, A2059
2FGLJ1506.6+0806	3.2	MKW35, A2063
2FGLJ1508.5+2709	3.8	A2065
2FGLJ1512.2+0201	6.0	A2029
2FGLJ1522.1+3144	12.8	A2065
2FGLJ1539.5+2747	2.4	A2065
2FGLJ1548.3+1453	4.8	A2147
2FGLJ1553.5+1255	3.5	A2147
2FGLJ1607.0+1552	1.8	A2147
2FGLJ1635.2+3810	5.6	A2199
2FGLJ1640.7+3945	2.8	A2199
2FGLJ1642.9+3949	2.2	A2199
2FGLJ1800.5+7829	11.5	A2256
2FGLJ1955.0-5639	4.0	A3667
2FGLJ2317.3-4534	2.7	S1101
2FGLJ2319.1-4208	3.7	S1101
2FGLJ2324.7-4042	8.5	S1101
2FGLJ2327.9-4037	0.5	S1101
2FGLJ2347.2+0707	4.1	A2657
2FGLJ2350.2-3002	3.1	A4038
2FGLJ2353.5-3034	4.4	A4038
2FGLJ2359.0-3037	4.4	A4038

Ferrari, C., Govoni, F., Schindler, S., Bykov, A. M., & Rephaeli, Y. 2008, Space Sci. Rev., 134, 93  
 Finke, J. D., Razaque, S., & Dermer, C. D. 2010, ApJ, 712, 238  
 Franceschini, A., Rodighiero, G., & Vaccari, M. 2008, A&A, 487, 837  
 Healey, S. E., Romani, R. W., Cotter, G., et al. 2008, ApJS, 175, 97  
 Hoekstra, H., Donahue, M., Conzelmann, C. J., McNamara, B. R., & Voit, G. M. 2011, ApJ, 726, 48

**Table A.2.** List of photon events within a circular region of  $0.3^\circ$  radius centered on A0119, A3112, A4038, A0400, 2A0335, A1367, MKW4, A2255, A2063, and A3581

Cluster name	Arrival time (MET), s	Energy, GeV
A0119	261033225	10.8
A0119	267864212	28.3
A0119	290446871	150.0
A3112	247100190	66.7
A3112	251029235	90
A3112	268175993	11.2
A4038	282124076	11.9
A4038	310302979	20.4
A4038	369147989	13.1
A0400	250037714	24.1
A0400	291576539	11.9
A0400	297933185	50.8
A0400	330823308	10.7
2A0335	283348255	11.7
2A0335	333270630	10.8
2A0335	352741781	36.8
2A0335	358456858	10.3
A1367	260628741	48.6
A1367	314405927	14.9
A1367	349727501	70
A1367	351437188	22.3
MKW4	241698944	14.3
MKW4	255282333	10.3
MKW4	263466545	10.9
MKW4	323071228	11.5
A2255	327382581	60
A2255	338658407	12.3
A2255	361107399	14.6
A2255	373040091	177.5
A2063	245663292	18.9
A2063	249511419	18.0
A2063	250975083	16.9
A2063	333842971	12.8
A2063	348468092	14.1
A3581	242221372	16.8
A3581	252236390	11.7
A3581	272025793	15.8
A3581	292681335	12.2
A3581	300957764	11.9

- Kneiske, T. M., Mannheim, K., & Hartmann, D. H. 2002, *A&A*, 386, 1  
Li, T.-P. & Ma, Y.-Q. 1983, *ApJ*, 272, 317  
Mattox, J. R., Bertsch, D. L., Chiang, J., et al. 1996, *ApJ*, 461, 396  
Michelson, P. F., Atwood, W. B., & Ritz, S. 2010, *Reports on Progress in Physics*, 73, 074901  
Miniati, F. 2003, *MNRAS*, 342, 1009  
Moiseev, A. A., Hartman, R. C., Ormes, J. F., et al. 2007, *Astroparticle Physics*, 27, 339  
Nolan, P. L., Abdo, A. A., Ackermann, M., et al. 2012, *ApJS*, 199, 31  
Peterson, J. R., Kahn, S. M., Paerels, F. B. S., et al. 2003, *ApJ*, 590, 207  
Peterson, J. R., Paerels, F. B. S., Kaastra, J. S., et al. 2001, *A&A*, 365, L104  
Petrosian, V., Bykov, A., & Rephaeli, Y. 2008, *Space Sci. Rev.*, 134, 191  
Pinzke, A. & Pfrommer, C. 2010, *MNRAS*, 409, 449  
Pinzke, A., Pfrommer, C., & Bergström, L. 2011, *Phys. Rev. D.*, 84, 123509  
Reimer, O., Pohl, M., Sreekumar, P., & Mattox, J. R. 2003, *ApJ*, 588, 155  
Reiprich, T. H. & Böhringer, H. 2002, *ApJ*, 567, 716  
Sarazin, C. L. 1986, *Reviews of Modern Physics*, 58, 1  
Thompson, D. J. 2008, *Reports on Progress in Physics*, 71, 116901  
Truemper, J. 1993, *Science*, 260, 1769  
Voges, W., Aschenbach, B., Boller, T., et al. 1999, *A&A*, 349, 389  
Völk, H. J., Aharonian, F. A., & Breitschwerdt, D. 1996, *Space Sci. Rev.*, 75, 279  
Wilks, S. 1962, *Mathematical Statistics* (New York: Wiley)  
Zimmer, S., Conrad, J., for the Fermi-LAT Collaboration, & Pinzke, A. 2011, *ArXiv e-prints* 1110.6863